MICROSTRUCTURAL FEATURES OF PRIMARY AND SECONDARY DUCTILE HIGH PRESSURE DIE CASTING ALLOYS FOR THE AUTOMOTIVE INDUSTRY

(A. Bakedano)
IK4-AZTERLAN, Engineering, R&D and Metallurgical Processes, Durango, Spain

(R. González-Martínez)
IK4-AZTERLAN, Engineering, R&D and Metallurgical Processes, Durango, Spain

(A. Niklas)
IK4-AZTERLAN, Engineering, R&D and Metallurgical Processes, Durango, Spain

(M. da Silva)
Fundació Privada Ascamm, Cerdanyola del Vallès, Spain
Universitat Autònoma de Barcelona, Cerdanyola del Vallès, Spain

(M. Garat)
IK4-AZTERLAN, Engineering, R&D and Metallurgical Processes, Durango, Spain

(A.I. Fernández-Calvo)
IK4-AZTERLAN, Engineering, R&D and Metallurgical Processes, Durango, Spain

ABSTRACT

Primary AlSi10MnMg alloy is the most widely used alloy for manufacturing of vacuum assisted high pressure die castings (VPDC) with high ductility requirements. In this alloy, die soldering is avoided by a high Mn level (0.5 - 0.6 wt. %) while Fe is kept low (< 0.2 wt. %). Such combination guarantees that the Al-Fe-Mn-Si intermetallic phases are of the α-$Al_{15}(FeMn)_3Si_2$ polyhedral or Chinese script type which is least harmful to the ductility. But the use of a secondary alloy allows to significantly reduction of the cost of the castings as the raw material is cheaper and also requires less energy for their manufacturing.

On the other hand, secondary alloys contain a higher amount of Fe, a common impurity, which also reduces die soldering but is detrimental to the ductility due to the formation of needle/platelet shaped β-Al_5FeSi phase. Microadditions based on Mn have been found to be effective in transforming the needle/platelet shaped β phases into Chinese script α- iron phases with a less harmful morphology even in relatively high Fe alloys.

In this work a secondary alloy with 0.60 % Fe and different Mn microadditions, has been cast in test parts with different wall thicknesses using VPDC technology. The effect of microadditions and wall thickness on the morphology, amount and size of intermetallic iron phases has been investigated using image analysis and compared to the corresponding AlSi10MnMg primary alloy**.** The results show that the cooling rate is an important factor to control the size and area fraction of the intermetallic iron compounds. The additions of Mn results in modification of the β-Al_5FeSi compounds into a less harmful Chinese script and/or fine α-iron compounds. However, an increase in the area fraction of the intermetallic compounds is observed.

Keywords: High pressure die casting, vacuum assisted, β-iron phases, α-iron phases secondary alloy, high ductility.

71st BILBAO 2014 WORLD FOUNDRY CONGRESS
Advanced Sustainable Foundry
19-21 May 2014 • Palacio Euskalduna, BILBAO

INTRODUCTION

Primary aluminum-silicon-magnesium alloys are by far the most widely used type in the manufacturing of safety parts for the automotive industry, such as suspension components and wheels, due to their excellent castability and good mechanical properties[1] which can be further improved by heat treatment: solution, followed by water quenching, followed by artificial aging T6 or T7. Until the introduction of thin walled structural parts in the 1990's, these safety critical components were mostly produced in Permanent Mould and sometimes in Sand or Squeeze casting. Conventional primary alloys mostly of the AlSi7Mg type, and sometimes with higher Si (9 to 11) appear best suited to these parts/processes.
The more recent structural castings, being extremely thin walled (of the order of 2.5 mm) and of rather great dimensions usually require the use of High Pressure Die Casting. As they must be defect free and heat treatable to attain the requested properties, ductility and weldability being the most difficult to achieve, vacuum must be applied as well as a combination of precautions relative to the die design, die lubricant, melt quality and shot profile.

Secondary alloys usually contain impurities or trace elements such as Fe, Cu, Zn, Mn, Cr etc. From these elements iron is the most deleterious one with regard to the ductility, due to its tendency to form brittle intermetallic phases such as β-Al_5FeSi phases. These phases are detrimental to the mechanical properties, especially ductility and also to the shrinkage behaviour, and must be kept at levels as low as possible. Therefore, secondary alloys are very seldom employed for the manufacturing of parts with high mechanical properties requirements. However, the use of recycled alloys brings potential cost and energy savings, and generates less CO_2 emission compared to primary aluminium production.

High pressure die casting (HPDC) is one of the most popular processes for the fabrication of parts for the automotive aluminium industry due to its high productivity. In HPDC molten aluminium is injected under high pressure into a die cavity. Conventional HPDC alloys are usually secondary alloy, in which iron is intentionally in the range of 0.8-1.1 wt. % in order to prevent molten metal soldering to the die[2-4]. However, conventional HPDC alloys and processes are not suitable for high ductility castings and safety parts due to the presence of β-Al_5FeSi phases. For this reason, the primary AlSi10MnMg alloys with a maximum iron content of 0.25 and high Mn to avoid die soldering were developed[5]. Nevertheless, the use of recycled alloys can reduce significantly the fabrication costs of a part by increasing die life, die manufacturing and maintenance make up more than 10% of HPDC cast.

It is well known that addition of elements such as Mn, Cr, Sr, Co, Be and Ca can neutralize the effect of the harmful iron phases by substituting them by iron compounds with a less harmful morphology. The effect of these micro-additions on the iron compounds has investigated by several authors[6-16]. Furthermore, the effect of cooling rate and other variables such as temperature gradient, apparent rate of solidification on the reduction in size, number and volume fraction of Fe-intermetallic compounds has been studied with great interest by several researchers[18-20]. However, the effect of alloying elements and cooling rate has not received much attention[21] in components produced by HPDC.
The present work investigates the effect of small additions of Mn and wall thickness and thus cooling rate on the morphology, size and area fraction of the intermetallic iron compounds of an AlSi10MnMg secondary alloy with high iron content. Wall thicknesses representative of the most common components produced by HPDC were selected for this study. The aim was to substitute the AlSi10MnMg primary alloys with high Mn content by less expensive secondary alloys with high iron content and moderate Mn content.

DESIGN OF EXPERIMENTS

A Buhler cold chamber high pressure die-casting machine with a 520 tonne locking force, a shot sleeve with an internal diameter of 60 mm and a stroke of 450 mm was used in the tests (Figure 1). In the first step of the injection process the plunger was constantly accelerated in order to reduce the gas entrapment during this phase. The velocity was kept constant in the second phase, filling the cavity of the die. The velocity was 3.5 m/s in order to ensure the filling of the section of 1 mm. The vacuum achieved inside of the die allowed also the good filling during this phase. In this case, the third phase, the compression phase, started when the plunger felt a backpressure. For each experiment, 40 kg of each alloy were melted in an electric furnace with a capacity of 60 kg. The alloys were modified using AlSr10 master alloy. The melts were poured at a temperature between 680 ºC and 710 ºC into the shot sleeve.

Figure 1: Equipments where the research was performed

The chemical compositions of the alloys used in this work are presented in Table 1. Alloy A is a typical primary AlSi10MnMg alloy for VPDC castings with a Mn content of 0.68 wt. % and low Fe content of 0.17 wt. %. Alloys B and C are secondary alloys with 0.58 wt. % of Fe and a Mn contents of 0.22 and 0.57 wt % respectively. The higher Cu and Zn content present in both alloys B and C in comparison to the primary variant, is typical of recycled aluminum. The three alloys have Sr addition for eutectic Si modification. Alloy A and B present a similar total Mn+Fe of 0.85 wt. % (alloy A) and 0.81 wt. % (alloy B).

The die was designed to fabricate a step test piece with sections of 1, 2, 4, 6, 10 and 15 mm. The step test piece is shown in Figure 2. The effect of wall thickness on the morphology and size of the iron compounds is established in the steps of 1, 4 and 6 mm by optical and scanning electron microscopy. The characteristics and chemical composition of the intermetallic iron compounds were examined using scanning electron microscopy (SEM) with an energy dispersive X-ray spectrometer (EDS).

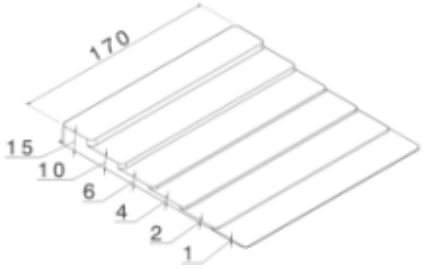

Figure 2. The step test pieces produced for the irrent evaluation. The measures are indicated in mm.

For the quantification of length and area fraction of both β and α iron compounds, twenty images were obtained at a magnification of 2000X. The plate length for the β compounds and the longest dimension for the α–compounds were measured, respectively. The area fraction and length of each compound was estimated using a LAS V4.2 image analyzer.

3. RESULTS AND DISCUSSION

3.1. EFFECT OF ALLOYING ELEMENTS ON THE MICROSTRUCTURE

The iron compounds formed in the 6 mm step of the test piece of the primary and secondary alloys are shown in the microstructures of Figure 3. The microstructure of the primary alloy (Figure 3a) consists of primary aluminium, eutectic Al-Si and compact intermetallic particles. The eutectic silicon cannot be distinguished from the aluminium in the scanning electron microscope due to the similar atomic weight of Al and Si. This facilitates the quantitative analysis of the iron rich compounds. In the microstructure of the primary alloy two sizes of α compounds can be observed. The large α compounds have a size between 10–16 µm and are probably primary phases which have formed in the shot sleeve, while the formation of the small particles α occurred during solidification in the die.

The secondary alloy with low Mn content (alloy B) reveals the formation of both fine α compounds and large β needles (Figure 3b). With the addition of Mn to this alloy, up to 0.58 wt % (alloy C in Figure 3c), the formation of β compounds was suppressed and instead small α (rounded and Chinese script) and large α compounds (Chinese script) appeared. The latter ones have a size of 50-75 µm and are probably primary phases that have been formed in shot sleeve. The results of the microstructure investigation show that as reported in literature Mn is an effective element in changing the β intermetallic compounds to Chinese script or polyhedral primary phase morphologies[8-10].

In alloy C, with an addition of Mn equal to the Fe content the β compound formation is completely avoided. However, the Mn addition probably could be reduced and should be optimized for the HPDC process regarding ductility. Indications about the best quantity to be added reported in literature are often not very precise and sometimes even contradictory[20]. One reason for this could be that the optimum addition also depends on the cooling rate. Some authors found that if the cooling rate is high enough the formation of β-Al_5FeSi can be minimised or even suppressed[8]. In addition to this, the magnesium content has also to be taken into account, because some iron present in the alloy will combine with Mg and form π Al-Fe-Si-Mg compounds.

Table 1. Chemical composition (wt. %)

Alloy	Si	Fe	Cu	Mn	Mg	Cr	Ni	Zn	Ti	Sr	Total Fe+Mn
A-Primary*	10.70	***0.17***	<0.01	***0.68***	0.47	<0.01	0.01	0.01	0.05	0.0061	0.85
B-Secondary low Mn	9.07	***0.58***	0.03	***0.22***	0.35	0.01	0.01	0.03	0.03	0.0195	0.81
C-Secondary high Mn	9.79	***0.58***	0.03	***0.57***	0.36	0.01	0.01	0.03	0.03	0.0218	1.16

*The primary alloy corresponds to the norm ENAC 43.500[22], Si: 9.0-11.5, Fe: 0.25, Cu: 0.05, Mn: 0.4-0.68 Mg: 0.1-0.6 wt. %.

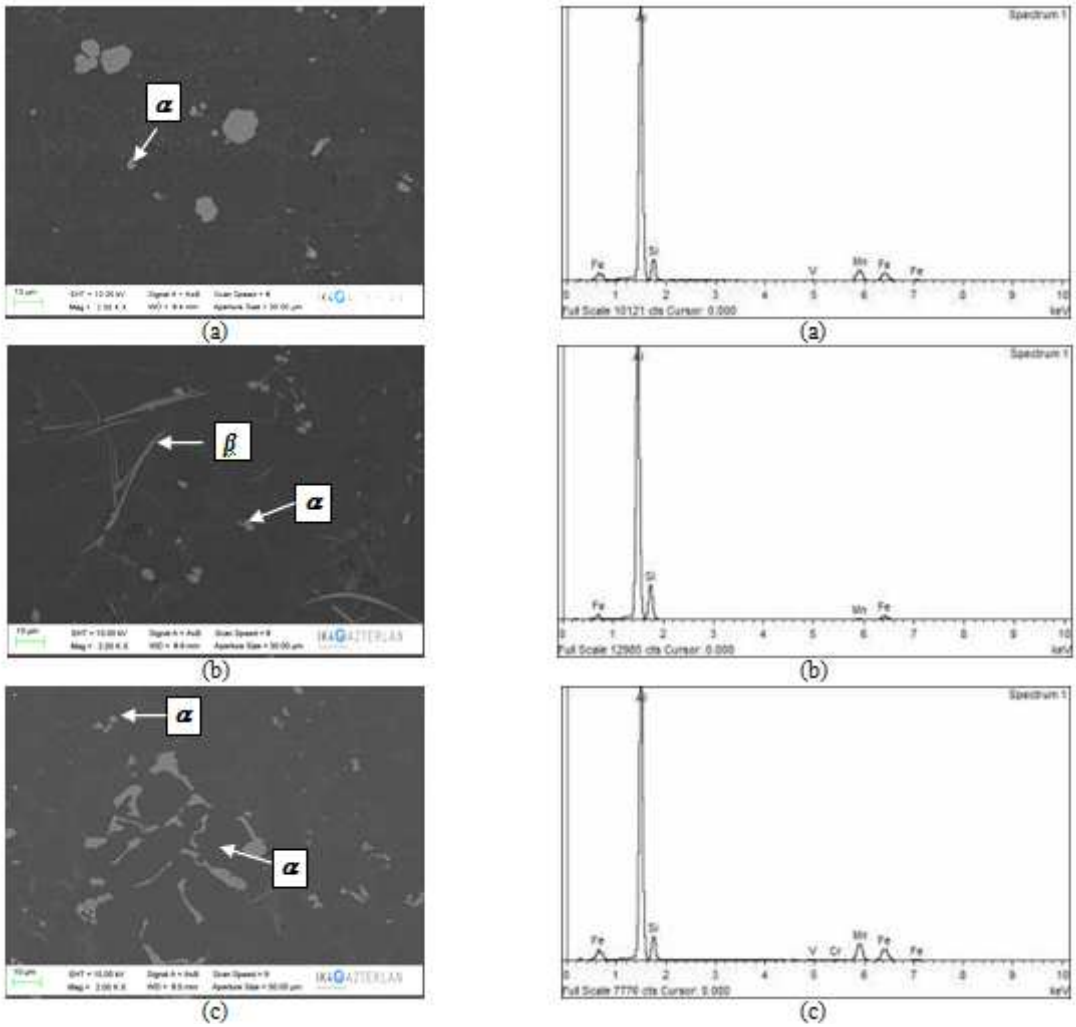

Figure. 3 Effect of alloying elements in the 6 mm step, microstructures and location of EDS analysis of the intermetallic iron compounds indicated with arrows: a) the primary alloy A, b) secondary alloy B with low Mn content and c) secondary alloy C with high Mn content.

The compositions of α and β compounds are summarized in table 2. It can be observed that all intermetallic compounds have Fe and Mn in their chemical composition. However, the Mn content in the β compounds of alloy B is very small in comparison with

the concentration in all α compounds. As the content of Mn increases in the alloy its quantity also increases in the analysed α compounds while the iron content decreases. It can be observed that the iron compounds of the secondary alloys contain small amounts of V, probably residual in the secondary alloy.

Table 2: Chemical composition of α and β compounds in wt. % determined by EDS analysis.

Alloy	Compound	Al	Si	Fe	Mn	V
A	α	75.4	11.4	2.2	11.0	–
B	β	72.2	19.5	6.7	1.5	–
	α	68.6	10.8	13.3	7.0	0.3
C	α	67.5	9.5	10.0	12.8	0.3

3.2 EFFECT OF WALL THICKNESS ON MICROSTRUCTURE

Figure 4 shows the microstructure of the steps with a wall thickness of 6, 4 and 1 mm for alloy A (primary alloy). The results of the image analysis are listed in Table 3. The microstructures of alloy A reveal a large and small polyhedral α iron compounds with a compact morphology in each analyzed step. No β intermetallic compounds are observed. It can be seen that the area fraction of small α particles decrease slightly by reducing the wall thickness. The large α particles have a similar size in each step between 10-16 µm (see Table 3). This confirms that the large ones have been formed in the shot sleeve. The reduction of the size of the small α particles can be explained by the fact that in the thin steps the cooling rate is higher than in the thick steps and hence nucleation rate for intermetallic particles is increased. This is in agreement with the investigation of Seifeddine[23] who also found that at higher cooling rate the amount, size and volume fraction of the intermetallic iron compounds were reduced in the alloy A390.

The effect of wall thickness on the intermetallic iron compounds of the steps with wall thicknesses of 6, 4 and 1mm of the secondary alloy with low Mn (alloy B) are shown in Figure 5 and Table 3. In this alloy coarse β-needles and fine intermetallic α compounds are formed. It can be clearly seen that the length and in particular the area fraction, of the β compound decreases significantly by decreasing the wall thickness. In the thinnest step only few β compounds are detected (area fraction of 0.07 %). Similar observations were made for the α compounds which show a decrease in length and area fraction when the wall thickness is reduced and hence cooling rate is increased. This effect is again attributed to higher solidification cooling rate present in the 1 mm step.

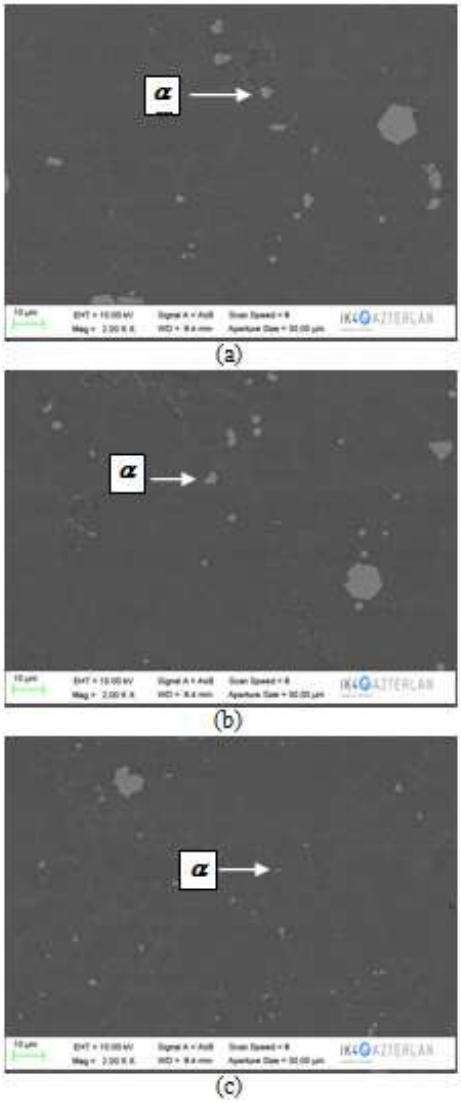

Figure. 4 Microstructures of the primary alloy with high Mn and low Fe content (alloy A) showing the effect of wall thickness on the intermetallic iron compounds in the steps of (a) 6 mm, (b) 4 mm and (c) 1 mm.

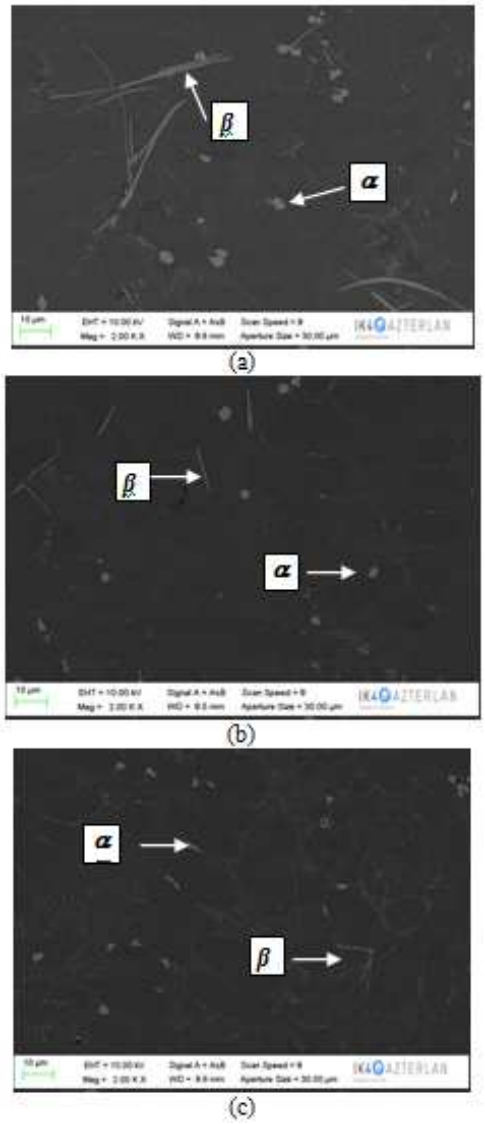

Figure 5. Microstructures of the secondary alloy with low Mn content (alloy B), showing the effect of wall thickness, (a) 6mm, (b) 4mm and (c) 1mm.

Figure 5 and Table 3 show the effect of wall thickness of the steps for secondary alloy C with a Mn content equal to the Fe content. Additions of Mn resulted in the formation of large Chinese script α compounds and small rounded or Chinese script α compounds. The large α Chinese script compounds have a similar size in each step between 50-75 μm. This indicates that the large ones have been formed in the shot sleeve. No β compounds are observed in none of the steps.

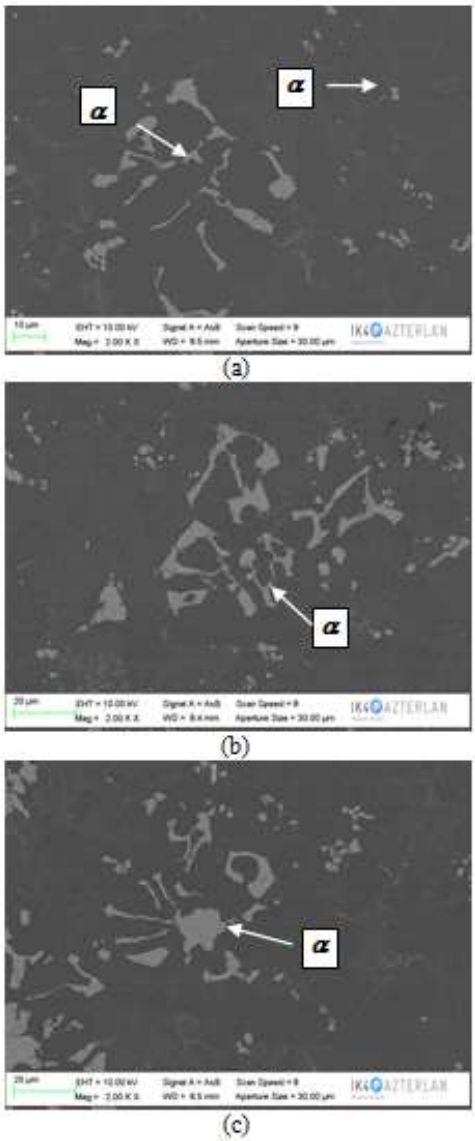

Figure 6. Microstructures of the secondary alloy with high Mn content (alloy C) showing the effect of wall thickness on the intermetallic iron compounds in the steps of (a) 6 mm, (b) 4 mm and (c) 1 mm.

The characterization of the intermetallic iron compounds of the three analyzed alloys are summarized in Table 3. The formation of β iron compounds is more affected by the reduction in wall thickness than the α iron compounds; in the step with the lowest wall thickness of 1 mm the nucleation is almost completely suppressed. However, also the size of α compounds is reduced by decreasing the wall thickness. Thus, the cooling rate is an

important factor to control the size of the β and α compounds obtained in the microstructure.

Table 3: Characteristics of the intermetallic iron compounds in the three alloys

Alloy	Step (mm)	β (µm)		α (µm)	Area Fraction	
		Average Length	Maximum Length	Average Length	A_β (%)	A_α (%)
A	6	-	-	3.3(*)1	-	1.56
	4	-	-	3.2(*)1	-	1.40
	1	-	-	2.6(*)1	-	1.20
B	6	13.81	42.0	4.0	0.60	0.74
	4	10.29	28.7	4.2	0.28	0.92
	1	7.58	12.8	3.4	0.07	0.43
C	6	-	-	2.9(*)2	-	2.70
	4	-	-	3.0(*)2	-	2.69
	1	-	-	2.9(*)2	-	2.42

(*)1 Coarse α compact particles of 10-16 µm are not considered.
(*)2 Chinese script coarse α particles of 50-75 µm are not considered.

Figure 7 shows the area fraction of all intermetallic iron compounds α and β in the steps of 6, 4 and 1 mm for the three studied alloys. It can be seen that the alloy B shows the lowest area faction of intermetallic iron compounds while alloys A (primary variant with high Mn content) reveals a slightly higher area fraction. The secondary alloy with high Mn presents the double area fraction when compared with the primary alloys. Thus, it will be necessary to optimize the Mn content in order to obtain the lowest amounts of intermetallics possible without forming harmful β compound. However, for avoiding die soldering high total amount of Fe plus Mn are desired.

Furthermore, a small decrease of area fraction with reduction of wall thickness is observed. Several authors observed the same decrease of area fraction when cooling rate increases, and they attributed this to a delay in the growth mechanism of the intermetallic iron compounds[24-26].

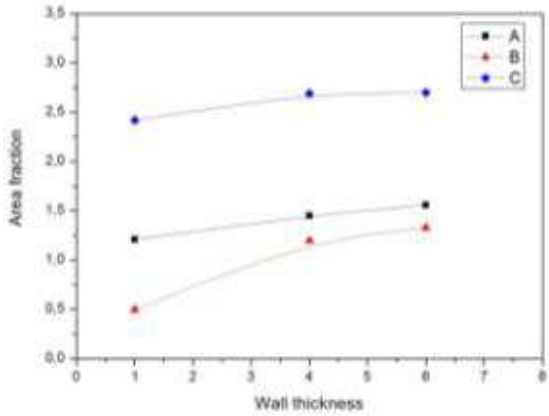

Figure 7. Effect of the alloying elements on the area fraction of the intermetallic iron compounds. Note: Both α and β compounds are included in the area fraction of alloy B.

CONCLUSIONS

The effect of different Mn microadditions to secondary alloys and wall thicknesses (cooling rates) on the morphology, particle size and the area fraction of intermetallic iron compounds has been investigated in step test parts and compared to the corresponding AlSi10MnMg primary alloy**.** The following conclusions have been drawn:

- A higher cooling rate, obtained in the thinnest walled step, results in an important reduction in size and total volume of the β-compounds, but much less so of the α-iron compounds. The formation of the β phase can be almost suppressed in the thinnest step with 1 mm.
- Additions of Mn are very effective to substitute the harmful β-Al_5FeSi compounds by Chinese script and/or fine α-iron compounds. However, with increasing Mn content also the size and area fraction of the α-iron compounds increase.
- It is believed that the largest α-iron compounds appear in the shot sleeve and that their size is largely controlled by the temperature and dwell time. A special attention should be given to the conditions in the shot sleeve, with a view to limiting as much as possible the precipitation at this step of the process.

Future work should also concentrate on determining the effect of morphology, particle size, and area fraction on the mechanical properties.

ACKNOWLEDGMENT

This research was financially supported by European Union´s Seventh Framework Programme managed by REA – Research Executive Agency under grant agreement nº **315506** (FP7-SME-2012-1).

The authors also wish to thank to Mr Enrique Vedia and Eulàlia Nogés for assisting on the operation of the HPDC machine at ASCAMM Technology Centre.

REFERENCES

1. Gruzleski, J., Closset, B. M., "The treatment of liquid aluminium-silicon alloys", American Foundry´s Society, IL (1990).
2. Belov, N.A., Aksenov, A.A., Eskin, D.G. Iron in aluminium alloys, Alloying Element, Taylor and Francis., New York (2002).
3. Apelian D. Shankar, Materials Transaction 33B pp. 465-476 (2002).
4. Shabestari, S.G., Materials Science Technology A383:289 (2004).
5. Koch, H., Hielscher U., Sternau H. Franke, A., "Silafont 36 high pressure die casting alloy", Light Metals 1995, TMS pp. 1011-1018 (1995).
6. Murali, S., Raman, K.S., Murthy, K.S.S, "Effect of trace additions (Be, Cr, Mn and Co) on the mechanical properties and fracture toughness of Fe-containing AlSi7Mg0.3 Alloy", Cast Met. Vol. 6, pp.189-198, (1994).
7. Sreeja Kumari, S.S., Pillai, R.M., Nogita, K., Dahle, A.K., Pai, B.C., "Influence of calcium on the microstructure and properties of an Al-7Si-0.3Mg-xFe alloy", Metallurgical and Materials Transactions. A, Vol. 37A, pp. 2581-2587, (2006).
8. Gustafsson, G., Thorvaldsosson, T., Dunlop, G.L., "The influence of Fe and Cr on the microstructure of cast Al-Si alloys", Metallurgical Transactions A, Vol. 17A, pp. 45-52, (1986).
9. Kim, H.Y., Han, S.W., Lee, H.M., "The influence of Mn and Cr on the tensile properties of A356–0.20Fe alloy", Materials Letter Vol. 60, pp. 1880-1883 (2006).
10. Lu, L., Dahle, A.K., "Iron-rich intermetallic phases and their role in casting defect formation in hypoeutectic Al-Si alloys", Metallurgical and Materials Transactions A, Vol. 36A, pp. 819-835, (2005).
11. Anantha Narayanan, L., Samuel, F. H., Gruzleski, J. E., " Crystallization behavior of iron-containing intermetallic compounds in 319 aluminum alloy", Metallurgical and Materials Transactions A Volume 25, Issue 8, pp. 1761-1773, (August 1994).
12. Samuel, A.M., Samuel, F.H., Doty, H.W., "Observations on the formation of β-Al5FeSi in 319 type Al-Si alloys", Journal of Material Science., Vol. 31, pp. 5529-5539, (1996).
13. Sigworth, G. K. Theoretical and Practical Aspects of the Modification of Al-Si. Modern Casting 77 No., pp.23-25 (1987).
14. Shabestari S. G., and Gruzleski J.E., "Modification of Iron Intermetallics by Strontium in 413 Aluminum Alloys", AFS Trans 103 pp. 285-293, (1995).
15. Ashtari, P; Tezuka, H; Sato, T, "Influence of Sr and Mn additions on intermetallic compound morphologies in Al-Si-Cu-Fe cast alloys" Materials Transactions, Volume**:** 44, Issue: 12, pp.2611-2616, (2003).
16. Shabestari, S. G., Keshavarz, M., Hejazi, M. M., "Effect of strontium on the kinetics of formation and segregation of intermetallic compounds in A380 aluminium alloy, Journal of alloys and compounds 477. pp. 892-899, (2009).
17. de la Fuente, E. E. Alfaro, I. Niklas, A. Anza I., Fernández-Calvo A.I., Improved microstructure and mechanical properties of a recycled AlSi7Mg0.3 alloy with 0.3 wt% Fe by small additions of Mn, Cr, and V. 8th Aluminium two thousand congress 14-18 Milano, Italy (May 2013).
18. Wang L., D. Apelian, Makhlouf, "Iron-Bearing compounds in Al-Si Die-casting alloys: Morphology and conditions under which they form" AFS Transactions 146 231-238 (1999).
19. Ma, Z. Samuel A.M. Samuel F.H., "Effect of iron and cooling rate on tensile properties of B319.2 alloys in non-modified and Sr-Modified conditions" AFS transactions 131-140 (2004).
20. Crepeau, P.N., "Effect of iron in Al-Si casting alloys: A critical Review", AFS transaction 103 pp. 361-366 (1995).
21. Kulunk, B., Shabestari, S G; Gruzleski, J E; Zuliani, D J, Transactions of the American Foundrymen's Society V 103 Paper 96-170 P 1189-1193, 1996.
22. Norm UNE-EN 1706:2011
23. Seifeddine, S., Svenssson, I.L., "The influence of Fe and Mn content and cooling rate on the microstructure and mechanical properties of A380-die casting alloys, Metallurgical Science and Technology, Vol. 27-1 pp. 11-20 (2009)
24. Espinoza-Cuadra, J., Gallegos-Acevedo, P., Mancha-Molinar H., Picado, "Effect of Sr and solidification conditions on characteristics of intermetallic in Al-Si

319 industrial alloys", Materials and Design 31 pp. 343-356 (2010).

25. Verma, A. Kumar S. Grant, P.S., O'Reilly K.A.Q. Influence of cooling rate on the Fe intermetallic formation in an AA6063 Al alloy", Journal of Alloys and Compounds 555 pp. 274-282, (2013).
26. Terzi, S., Taylor, J.A., Cho, Y.H., Salvo, L., Suéry, M., Boller, E., Dahle A.K., In situ study of nucleation and growth of the irregular α-Al/β-Al_5FeSi eutectic by 3-D synchrotron X-ray microtomography, Acta Materialia, Volume 58, Issue 16, pp 5370-5380 (September 2010).